Thermochimica Acta 486 (2009) 27–31

Contents lists available at ScienceDirect

Thermochimica Acta

journal homepage: www.elsevier.com/locate/tca

Composition dependence of the solid state transitions in $NaNO_3/KNO_3$ mixtures

Wen Ping[a], Peter Harrowell[a,*], Nolene Byrne[b], C. Austen Angell[b]

[a] School of Chemistry, University of Sydney, Sydney 2006, Australia
[b] Department of Chemistry, Arizona State University, Tempe, AZ 85287-1604, USA

ARTICLE INFO

Article history:
Received 11 July 2008
Received in revised form 14 October 2008
Accepted 15 December 2008
Available online 24 December 2008

PACS:
64.70.kp
65.40.Ba

Keywords:
Alkali nitrate
λ-Transition
Solid state calorimetry

ABSTRACT

The results of a detailed calorimetric study of the $NaNO_3/KNO_3$ phase behaviour as a function of cation composition are presented. We conclude that the λ-transition in $NaNO_3$ is significantly depressed and broadened by the presence of K^+ ions. The α–β-transition in KNO_3 is similarly affected. The possibility is considered that the depression of the λ-transition by addition of solute K^+ ions is related to random field effects on model lattice transitions involving a continuous order parameter. Some brief remarks are made to contrast the fast ordering kinetics of the λ-transition with the slow kinetics, and structural arrests, obvious in supercooling liquids.

1. Introduction

The coupling of orientational degrees of freedom to structural fluctuations is an essential component of molecular liquids and solids. The details of this coupling, however, remain poorly resolved. A striking example of the role of molecular orientations in a collective transition is provided by the λ-transition that occurs in $NaNO_3$ crystals at a temperature 30 °C below the melting point. This well-studied phenomenon is associated with the order–disorder transition of nitrate orientations in the crystal lattice. In this paper we shall study how this 'simple' transition is perturbed by the introduction of solute disorder in the lattice in the form of K^+ ions. This perturbation represents a coupling between the orientational degrees of freedom and the structural fluctuations as discussed above.

In spite of the extensive literature on the binary salt system $NaNO_3/KNO_3$, its phase diagram has proved remarkably difficult to pin down [1–8]. The debate has revolved around the question of whether the solidification should be described as a typical eutectic process (three-phase equilibrium) or, instead, as a rather atypical two-phase transition to a solid solution [8]. Recent measurements of the electrical conductivity of the solidified 50:50 mole% composition and of the melting enthalpy have suggested that the solid consists of alternating areas of sodium nitrate-rich and potassium nitrate-rich composition [6,9]. Raman microscopy of the equimolar mixture has confirmed the presence of Na- and K-rich domains of roughly 3 μm diameter [8]. Berg and Kerridge [8] have argued that these results provide strong support for the presence of a eutectic mode of crystallization. This conclusion is in clear contrast to that of Greis et al. [5] and Xu and Chen [7] who, based on calorimetric evidence and Raman spectroscopy, respectively, concluded that the $NaNO_3/KNO_3$ phase diagram exhibited a solid solution at low temperature. The authors of ref. [8] suggested that the previous studies [5,7] had not allowed sufficient time for equilibration.

Berg and Kerridge [8], in arguing for the existence of the eutectic, did not propose a modified phase diagram nor explicitly address the composition dependence of the solid state phase transitions. While our primary goal in this paper, as stated above, is to characterize experimentally the effect of translational disorder of solute ions on the rotor transitions, we shall inevitably need to address these alternate versions of the equilibrium behaviour of the low temperature mixture.

2. Crystal structures of $NaNO_3$ and KNO_3

The phase diagram of potassium nitrate KNO_3 [9] indicates that two solid phases, α and β, can be observed at an atmosphere pressure (although a triple point involving the γ phase exists at slightly higher pressures). At low temperatures (e.g., room temperature), the stable phase is the α-KNO_3 structure. α-KNO_3 has an orthorhombic $Pmnc(D_{2h})$ space group with $Z=4$ (where Z is the number of formula units in the primitive cell) [10,11]. The nitrate

* Corresponding author.
E-mail address: peter@chem.usyd.edu.au (P. Harrowell).

0040-6031/$ – see front matter © 2008 Elsevier B.V. All rights reserved.
doi:10.1016/j.tca.2008.12.017

ions lie in the plane perpendicular to the *c* axes of the unit cell (as they do in all the crystal structures we deal with in this paper). Moving parallel to the *c* axes, the nitrate orientations alternate regularly between two orientations rotated by 60° from one another [12]. On heating, α-KNO_3 transforms into β-KNO_3 at ∼127 °C. β-KNO_3 represents a different crystal structure, the rhombohedral $R\bar{3}m$ space group with $Z=3$, and the nitrate ions exhibit orientational disorder within the plane perpendicular to the *c* axes. This disorder has been described as the random choice of two orientations differing by 60°. Simulation studies [13] indicate that this 'two-state' disorder is accompanied by a significant increase of rotational fluctuations in the plane compared to that found in the α phase, sufficient to warrant treating the NO_3^- as free rotors.

On cooling, β-KNO_3 is observed to undergo a transition at ∼124 °C, not into the stable α-KNO_3 phase, but, instead, into the metastable ferroelectric phase, γ-KNO_3 [10–12]. This phase has a similar crystal structure to that of the β phase (the unit cell length along the *c* axes is slightly shorter in the γ phase as compared to the β phase). The main difference between the two phases is that in γ-KNO_3 there is orientational order of the nitrates in the plane. This order, however, is not global. Different layers of unit cells perpendicular to the *c* axes can adopt either one of the two distinct nitrate orientations. The transition from γ to α is a slow transition and sensitive to the thermal history [13], with the γ phase able to persist indefinitely at room temperature.

$NaNO_3$ exhibits two solid phases under atmospheric pressure [14]. At room temperature, the equilibrium state of $NaNO_3$ is an ordered calcite structure in the trigonal $R\bar{3}c$ space group with $Z=2$ [7]. On heating, the crystal undergoes a second order λ-like transition near 276 °C into a structure of average trigonal $R\bar{3}m$ space group with $Z=1$. This is a calcite structure in which the nitrate ions exhibit rotational disorder in the plane normal to the c axis. The orientations of the NO_3^- ions are continuous with six preferred calcite-type orientations above the phase transition temperature [15]. The crystal melts at 307 °C.

There is no evidence of any significant change in translation order or mobility of the ions accompanying the orientational transitions in $NaNO_3$. For example, the electrical conductivity of $NaNO_3$ drops abruptly from ∼0.3 Scm^{-1} to 10^{-5} Scm^{-1} on freezing [6] into the orientationally disordered state with no further significant change in conductivity occurring as the material is cooled through the λ-transition. This result indicates that (i) the ions are relatively immobile in the plastic phase and (ii) there is no discernable change in ion mobility at the λ point.

3. Materials and methods

Reagent grade $NaNO_3$ and KNO_3 from Sigma–Aldrich were used without further purification. Our measured transition temperatures for melting and the α–β-transition in $NaNO_3$ and KNO_3 were in good agreement with literature values [6,8]. The thermal analyses were carried out on a Mettler Toledo DSC823^e thermal analyzer. The compositions were determined by weighing carefully dried salts (drying involved holding the sample at 250 °C for 24 h). The DSC samples (15–25 mg) were placed in sealed aluminum pans. Unless otherwise indicated, a scan rate of 20 °C/min was used for heating and cooling. References to a "liquid N_2 quench" refer to immersing the molten sample (in the sealed pan) directly into liquid N_2 to affect a very rapid cooling.

4. Results

In Fig. 1a we plot the heat flow vs. temperature of a range of $NaNO_3$/KNO_3 mixtures (where *x* is the mol percentage of KNO_3)

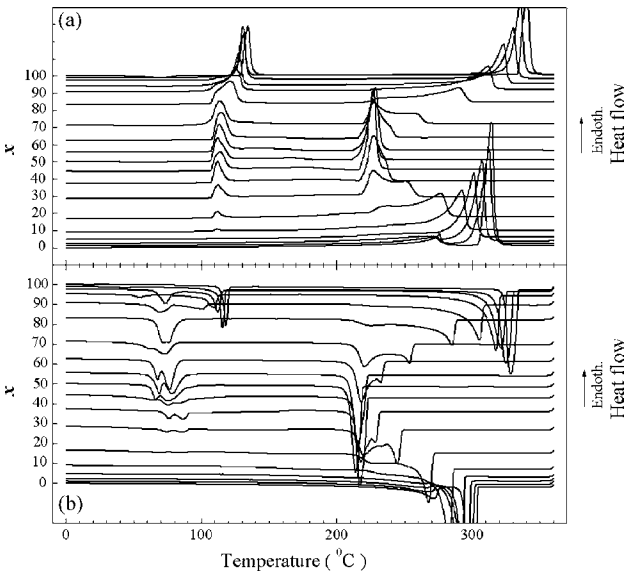

Fig. 1. The DSC curves for the compositions of $xKNO_3(100-x)NaNO_3$ ($0 \le x \le 100$) measured during heating at 20 °C/min (a) and during cooling at 20 °C/min (b).

during DSC upscan at 20 °C/min. The samples were prepared by cooling from 360 °C to −100 °C at 20 °C/min. The heat flow associated with this cooling process was also measured (see Fig. 1b). In the heating curves (Fig. 1a) an endothermic peak is prominent at 112 °C for most of the composition range (i.e. 3% < *x* < 95%). As we approach the pure KNO_3 limit this peak broadens and then sharpens up and shifts up to ∼127 °C. This transition corresponds to the transformation of α-KNO_3 into β-KNO_3 [12]. The cooling curves (Fig. 1b) show a quite different picture. In pure KNO_3 (i.e. $x=100$) a sharply peaked exotherm appears at ∼124 °C, which has been attributed to the transformation of β-KNO_3 into metastable γ-KNO_3 [12].

The effect of the KNO_3 addition into $NaNO_3$ on the λ-transition is shown in Fig. 2. The DSC curves in Fig. 2 are the same as shown in Fig. 1a, but the composition scale is expanded. Up to 3% KNO_3, the λ-transition peak exhibits a substantial broadening and the position of the peak T_{max} exhibits a small decrease with increasing concentration of K^+. As this broadening increases further at 5% KNO_3, the transition appears to resolve itself into two broad peaks. One remains at roughly the transition temperature of pure $NaNO_3$ and is lost as the depression of the melting transition obscures it.

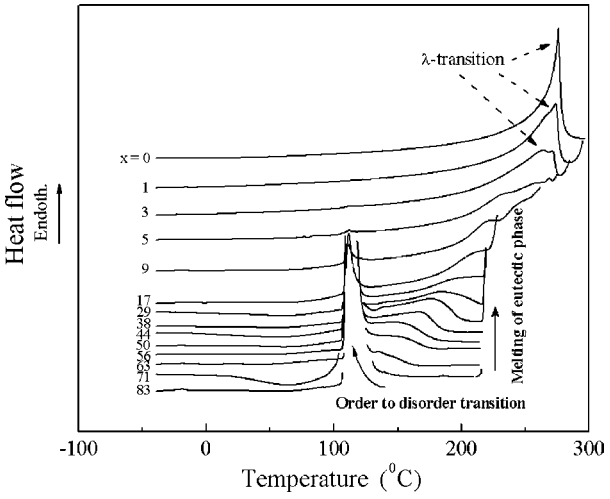

Fig. 2. The DSC curves of the compositions with $xKNO_3(100-x)NaNO_3$ ($0 \le x \le 83$) measured during heating at 20 °C/min.

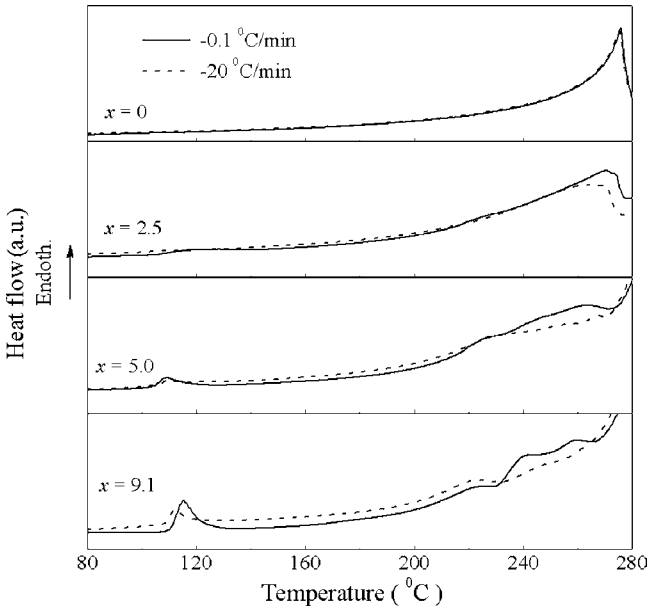

Fig. 3. The DSC curves associated with the λ-transition obtained by heating at 20 °C/min for samples prepared by cooling at 20 °C/min and 0.1 °C/min. The composition range covers 0 to 9.1% KNO_3.

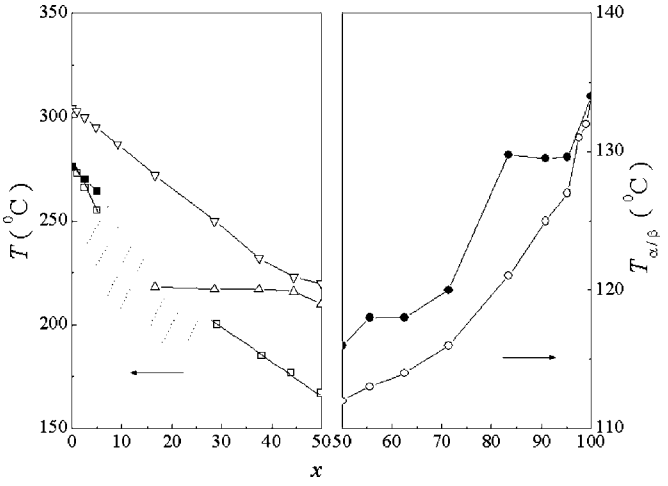

Fig. 5. Notable features of the DSC scans (shown in Fig. 1) plotted in the $T-x$ plane. The inverted triangles (▽) correspond to the onset temperature of crystallization as seen during cooling. The triangles (Δ) correspond to the onset temperature of melting during heating runs. The squares correspond to the λ-transition during heating (the dashed-line region contains the composition range over which the solid state transition is obscured by the solid–liquid transition). The diamonds correspond to the α to β-transition as seen on heating. Note the different temperature scales for the left and right sides of the plot.

The second and lower temperature peak proceeds to move steadily to even lower temperatures with increasing K^+ concentration until it becomes obscured by the endotherm resulting from the α to β-transition of KNO_3 at 118 °C.

In light of the warning expressed by Berg and Kerridge [8] concerning equilibration, we have compared in Figs. 3 and 4 the DSC scans on heating for samples prepared by cooling at 0.1 °C/min, 20 °C/min and, in the case of the K-rich samples, very rapidly with a liquid N_2 quench. (In ref [8], a cooling rate of 0.1 °C/min was used.) In Fig. 3, we look at the λ-transition in Na-rich samples. While the slower cooling rate is found to produce sharper features during the subsequent heating scan, we find little significant difference between the two cooling rates. In contrast, the cooling rate does influence the DSC scans in the K-rich solids as shown in Fig. 4. As in the case of the Na-rich solid, the slower cooling rate produces sharper features in the heating scans. Now, however, there is also a significant increase in the temperature of the α–β-transition for the slower cooling, except for the case of the pure KNO_3 sample. The most striking difference in peak temperatures between the sample cooled at 20 °C/min and that cooled at 0.1 °C/min occur around the composition of 80% KNO_3 where, in Fig. 4, we see the a much broader peak in the more rapidly cooled sample. We conclude that compositional fluctuations are the origin of the slow relaxation process. In considering why such fluctuations do not appear to influence the λ-transition, we note that the latter transformation takes place roughly 130 °C higher in temperature than the transition between α-KNO_3 and β-KNO_3.

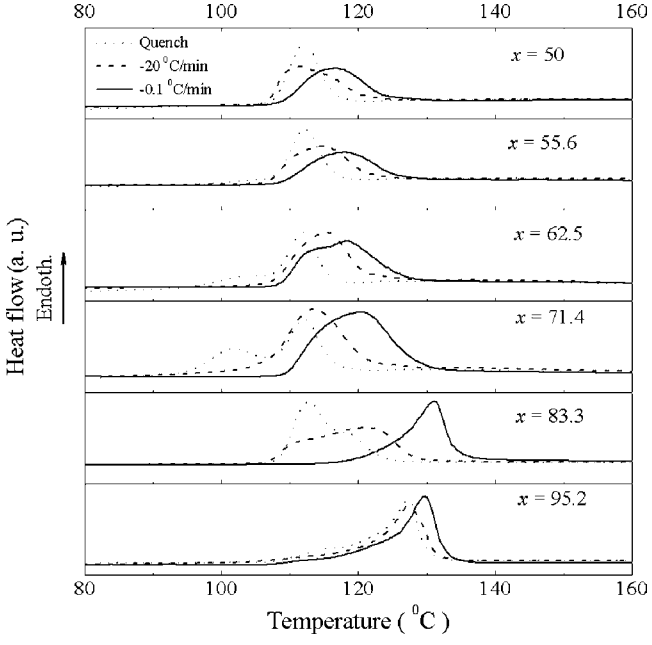

Fig. 4. The DSC curves associated with the α–β-transition obtained by heating at 20 °C/min for samples prepared by cooling at 20 °C/min, 0.1 °C/min and very rapidly using a liquid N_2 quench. The composition range covers 50–95.2% KNO_3.

The composition dependence of the main features of the DSC scans on heating are plotted in Fig. 5. The data from the 0.1 °C/min cooling runs are included. In the Na-rich side of the phase diagram we include the solidus and liquidus curves as we have been able to resolve them. Both solid state transitions exhibit a continuous variation with concentration. In the case of the Na-rich solids, the melting transition overlaps the λ-transition sufficiently to prevent us being able to unequivocally trace its dependence on potassium concentration beyond ∼5% KNO_3. However, even over this limited range, we can clearly see a substantial decrease in the transition temperature with increasing KNO_3. The α–β-transition in the K-rich solid also exhibits a significant depression as one moves away from the pure solid, although the 0.1 °C/min cooled sample presents us with a concentration independent peak (see Figs. 4 and 5) over the composition range 80–90% KNO_3. The observation of these continuous variation of the solid state transition temperatures with composition strongly points to the presence of phases with continuously varying composition. (An alternative possibility is that the transition associated with this persistent peak is influenced by finite size of the domains and that, as the domain size changes with composition, so does the transition temperature.)

In Fig. 6 we present a more detailed study of the transition up to 3% KNO_3 determined during heating. (Note the appearance of the low temperature shoulder discussed in the previous paragraph.) Over this narrow composition range the peak remains well defined

Table 1
The excess entropy change ΔS_{ex}, as defined in the text, arising from the rotation of nitrate ions at different concentrations of KNO_3 in the $KNO_3/NaNO_3$ mixture determined at a temperature where the heat capacity has a minimum between the λ-transition and melting process.

Mole fraction of KNO_3	0	0.005	0.01	0.015	0.02	0.025	0.03
ΔS_{ex} ($J\,mol^{-1}\,{}^{\circ}C^{-1}$)	30.5	28.0	26.5	27.2	26.9	27.0	27.3
T (°C) at which ΔS_{ex} determined	288	285	280	277	276	275	273

and questions concerning the global character of the equilibrium phase diagram do not enter since, in either proposal, we are considering a solid solution over this composition range. In seeking to understand the role of the solute on the rotor transition we would like to know whether the broadening of the transition peak is associated with a loss of degrees of freedom (e.g., by solute pinning of nitrate rotations). To address this question we have calculated an excess entropy ΔS_{ex} defined as the integral

$$\Delta S_{ex} = \int_{T_o}^{T_1} dT \frac{[C_P(T) - C_{\mathrm{Debye}}(T)]}{T} \quad (1)$$

$C_P(T)$ is determined by dividing the measured heat flow by the temperature scan rate and the sample mass. $C_{Debye}(T)$ is the heat capacity of the translational degrees of freedom calculated using values of the Debye temperature of 453 K and of the number of atoms being 5. T_0 is 20 °C, below which $C_P(T) \approx C_{\mathrm{Debye}}(T)$. T_1 is the minimum in the measured heat capacity between the λ peak and that of the melting transition. Our calculated C_{Debye} is plotted in Fig. 6. The values of ΔS_{ex} vs. composition are provided in Table 1. The excess entropy of pure $NaNO_3$ comes to 0.533 of the value estimated for ideal NO_3^- rotors in the plane at 288 °C, suggesting that even above the transition, the rotors are not free but hop between a discrete number of orientations. As we increase the amount of K^+ ions up to 1% we find that ΔS_{ex} decreases by about 13% while further increases in dopant concentration above 1% do not produce any further change. In light of the small decrease in ΔS_{ex} due to the addition of solute we conclude that while the impurities result in a modest amount of pinning of nitrate rotations, the main effect of the K^+ is to produce inhomogeneous variations in the characteristic temperature of the rotor transition, resulting in the observed broadening. Given the small concentrations involved, these perturbations appear to have rather long range influence.

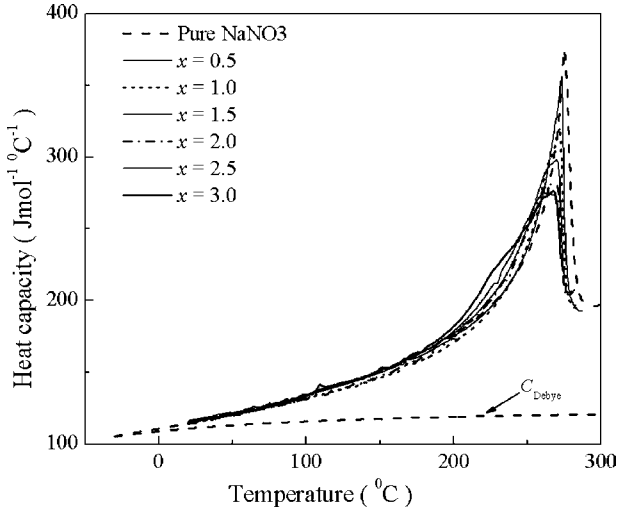

Fig. 6. The temperature dependence of the heat capacity of $xKNO_3(100-x)NaNO_3$ ($0 \le x \le 3$) determined by the DSC measurements during continuous heating runs. The dash line marked is Debye heat capacity of $NaNO_3$ deduced from Debye temperature of 453 K.

5. Discussion

In this paper we have characterized the substantial depression of the solid state transitions in $NaNO_3$ and, to a lesser extent, KNO_3 through the addition of a solute. The translational disorder associated with this solute substitution also broadens the transition (as measured by the heat flow rate peak). While we have found some evidence of a dependence of the solid state exotherms on cooling rate, we continue to see a continuous dependence on composition for both the λ-transition of $NaNO_3$ and the β to α-transition of KNO_3 at the same cooling rates at which Berg and Kerridge [8] report seeing segregation of the equimolar mixture. Acknowledging that this leaves the complete equilibrium phase diagram for the $NaNO_3/KNO_3$ mixture unresolved we consider the effect of solute disorder on the λ-transition of $NaNO_3$. For our purposes, the remaining uncertainty about the phase diagram means that we cannot assume that the solute distribution in a phase is an equilibrium one. The relaxation of the nitrate orientations, however, does appear to occur quite rapidly. (We cannot, for example, 'trap' the rotors in a nonequilibrium glass state even with a fast quench directly into liquid N_2.) For this reason, we believe that the rotors *do* come into equilibrium with whatever solute disorder they are presented with.

Our results suggest that solute disorder can substantially depress the rotor transition. This conclusion finds support in calorimetric data from the binary system $NaNO_3$–$AgNO_3$. Due to the similarity of Na^+ and Ag^+ radii, $AgNO_3$ can dissolve in the calcite structure of $NaNO_3$ over the range 0–32 mole% [16]. In this system, therefore, we have an equilibrium solid solution for a wide composition range. Starting from pure $NaNO_3$, the λ-transition persists but moves systematically to lower temperatures and smaller disordering entropies [17] as the Ag^+ concentration is increased. The scale of the transition temperature depression is similar to that observed in this present study due to the addition of K^+. One important difference between Ag^+ and K^+ as solutes in $NaNO_3$ is that in the Ag^+ system the composition dependence of the λ-transition follows that of the liquidus while in the K^+ system the solid state transition shows a much larger dependence on composition than the liquidus.

There exists a considerable theoretical literature on the effect of disorder on continuous order–disorder transitions with experimental realizations including disordered superconductors, randomly pinned spin density waves and crystalline surfaces with a disordered substrate (see ref. [18], and references therein). A well-studied model is the random field XY model in which dipoles with continuous rotational degrees of freedom interact with nearest neighbours only. The application of a random field on lattice models of spins results in the depression of the transition temperature. At a sufficiently large strength of the random field the order–disorder transition temperature goes to zero and the transition is completely suppressed [19,20]. It remains to be seen whether the rotor transition in solid solutions reported on here can be described by random field models.

It is characteristic of the order–disorder type of transition that the ordering kinetics are fast, essentially barrier-free, so that the loss of entropy from the ordering structure during cooling is not interrupted, as in the case of the entropy loss from a cooling liquid, by a glass transition. Very refined heat capacity measurements have been able to identify structural order arrests, but only at very low

temperatures e.g., 40 K for $CsNO_2$ (T_λ = 209.2 K) and 60 K for $TlNO_2$ (T_λ = 282.4 K) [21] where there is essentially no excess heat capacity left to lose. Unfortunately it is beyond the capacity of a DSC to detect this sort of structural arrest. It is of interest that the general rule has exceptions, the case of Co–Fe alloy being outstanding with a glass transition at $\sim 0.78T$ and a large jump in heat capacity [22]. It would be valuable to know whether the smearing of the λ-transition caused by the introduction of incompatible second components, like K^+ into the present $NaNO_3$ structure, affects the ordering kinetics in a significant way.

Acknowledgement

This research has been supported by a Discovery grant from the Australian Research Council.

References

[1] W.M. Madgin, H.V.A. Briscoe, J. Chem. Soc. 123 (1923) 2914–2916.
[2] C.M. Kramer, C.J. Wilson, Thermochim. Acta 42 (1980) 253–264.
[3] P. Nguyen-Duy, E.A. Dancy, Thermochim. Acta 39 (1980) 95–102.
[4] B.P. Ghost, K. Nag, J. Therm. Anal. 29 (1984) 433–437.
[5] O. Greis, K.M. Bahamdan, B.M. Uwais, Thermochim. Acta 86 (1985) 343–350.
[6] E.I. Eweka, D.H. Kerridge, Phys. Lett. A 174 (1993) 441–442.
[7] K. Xu, Y. Chen, J. Raman Spect. 30 (1999) 173–179;
E.I. Eweka, D.H. Kerridge, Phys. Lett. A 174 (1993) 441–448.
[8] R.W. Berg, D.H. Kerridge, Dalton Trans. (2004) 2224–2229.
[9] E.M. Levin, C.R. Robbins, H.F. McMurdie, Phase Diagrams for Ceramists Supplement, American Ceramic Society, Columbus, 1969, fig. 2799.
[10] D.M. Newns, L.A.K. Staveley, Chem. Rev. 66 (1966) 267–278.
[11] A.N. Christensen, P. Norby, J.C. Hanson, S. Shimada, J. Appl. Cryst. 29 (1996) 265–269.
[12] B.V. Schønwandt, H.J. Jakobsen, J. Solid State Chem. 145 (1999) 10–14.
[13] J.K. Nzmno, B.W. Lucas, Acta Cryst. B32 (1976) 1968–1971.
[14] H.M. Lu, J.R. Hardy, Phys. Rev. B 44 (1991) 7215–7224.
[15] E.M. Levin, C.R. Robbins, H.F. McMurdie, Phase Diagrams for Ceramists, vol. 2, American Ceramic Society, Columbus, 1969, fig. 4685.
[16] J. Liu, C.G. Duan, M.M. Ossowski, W.N. Mei, R.W. Smith, J.R. Hardy, Phys. Chem. Miner. 28 (2001) 586–590.
[17] S. Egolf, M.Sc. Thesis, Purdue University, 1969.
[18] T. Garel, G. Iori, H. Oland, Phys. Rev. B 53 (1996) R2941–2944.
[19] Y. Imry, S.-K. Ma, Phys. Rev. Lett. 35 (1975) 1399–1401.
[20] O. Kapikranian, B. Berche, Y. Holovatch, Eur. Phys. J. B 56 (2007) 93–105.
[21] K. Moriya, T. Matsuo, H. Suga, J. Phys. Chem. Solids 44 (1983) 1121–1132.
[22] H. Sato, H. Kikuchi, Acta. Metall. 24 (1976) 797–809.